Journal of Controlled Release 132 (2008) 65–73

Contents lists available at ScienceDirect

Journal of Controlled Release

journal homepage: www.elsevier.com/locate/jconrel

Layer-by-layer assembly of biologically inert inorganic ions/DNA multilayer films for tunable DNA release by chelation

Fuan Wang [a,b], Jianlong Wang [a,b], Yueming Zhai [a,b], Gaiping Li [a,b], Dan Li [a], Shaojun Dong [a,*]

[a] State Key Laboratory of Electroanalytical Chemistry, Changchun Institute of Applied Chemistry, Chinese Academy of Sciences, Changchun, Jilin 130022, PR China
[b] Graduate School of the Chinese Academy of Sciences, Beijing 10039, PR China

ARTICLE INFO

Article history:
Received 22 April 2008
Accepted 20 August 2008
Available online 4 September 2008

Keywords:
Layer-by-layer
Controlled release
Localized gene delivery
Chelation
Surface plasmon resonance

ABSTRACT

In this work, we illustrate a simple chelation-based strategy to trigger DNA release from DNA-incorporated multilayer films, which were fabricated through the layer-by-layer (LbL) assembly of DNA and inorganic zirconium (IV) ion (Zr^{4+}). After being incubated in several kinds of chelator solutions, the DNA multilayer films disassembled and released the incorporated DNA. This was most probably due to the cleavage of coordination/electrostatic interactions between Zr^{4+} and phosphate groups of DNA. Surface plasmon resonance (SPR), UV–vis spectrometry and atomic force microscopy (AFM) were used to characterize the assembly and the disassembly of the films. By incorporating plasmid DNA (pDNA) into this controllable disassembly system, the multilayer films sustained the consecutive DNA release. The released pDNA retained its integrity and transcriptional activity, and also expressed enhanced green fluorescent protein (EGFP) after being transfected into HEK 293 cells. Besides the simplicity and cost efficiency of this method, the most advantage of this route was that the release of DNA from the films could be modulated by various external conditions, such as the chelator and ionic strength. The Zr^{4+}/DNA multilayer films with the ability to precisely control the release rate of DNA might serve as an alternative localized gene delivery system in the perspective of biomedical applications.

1. Introduction

Gene therapy is defined as the administration of genetic material to modify or manipulate the expression of a gene product or to alter the biological properties of living cells for therapeutic use [1]. As a prerequisite for gene therapy, tunable and efficient gene delivery has been intensively pursued, not only for fundamental scientific interests but also for many potential clinical medicine applications. Furthermore, methods for the delivery of drugs from surfaces have an enormous clinical impact, and several feasible methods have been established for localized drug delivery. Recently, layer-by-layer (LbL) self-assembly technique has been receiving increased attention because of its potential as a simple, yet powerful, approach for constructing the building blocks of different compositions into ultrathin multilayer films with controlled thickness on essentially arbitrary solid substrates [2–5]. A wide variety of natural biomolecules and synthetic polyions have been incorporated into the LbL films via electrostatic interaction [6–9]. LbL thin films have been investigated extensively for tunable drug delivery applications based on the hypothesis that their highly tunable properties might lead to the controllable drug or gene release behaviors [10–19]. However, many challenges still exist, notably the development of improved systems that are versatile, highly responsive and effective to provide simple tunable drug or gene delivery for localized gene therapies. This is due, at least in part, to the lack of materials and approaches that are used to provide spatial and temporal control over the release and delivery of DNA and other nucleic acid-based therapeutics from surfaces.

The application of tunable gene delivery requires that the disassembly of the LbL films be controlled by external conditions. To meet this requirement, several methods have been developed toward the tunable gene release. As far as the degradation mechanisms are concerned, two strategies have been applied for tunable gene delivery. One is polycation-nondestructive way where the DNA-polycation interactions are weakened or broken by changing external conditions, such as pH [11], ionic strength [12] and redox potential gradients [13–16]. Unfortunately, the disassembly is reported to require changes in ionic strength or pH that is significantly outside the physiological range. Another attractive way is polycation-destructive way where the polycation is hydrolytically [17] or enzymatically [18] degraded and thus the incorporated DNA released. A newly established strategy utilizing the reduction of disulfide bonds in the backbone of the natural polypeptide or synthetic polycations also belongs to this mechanism [19]. The hydrolytically degradable polycations are very useful for sustained drug and gene delivery, but they degrade slowly during the preparation and storage of the LbL films. The enzymatically degradable polycations can overcome the obstacle in combination

* Corresponding author. Tel.: +86 431 85262101; fax: +86 431 85689711.
E-mail address: dongsj@ciac.jl.cn (S. Dong).

0168-3659/$ – see front matter © 2008 Elsevier B.V. All rights reserved.
doi:10.1016/j.jconrel.2008.08.016

with the advantages of good biocompatibility, high stability and precise tunable gene delivery. However, a suitable type of enzyme is required for their practical applications. The potential applications of this strategy would be limited because of the lack of suitable enzymes in some targeted tissues or organs of the human body. All these limitations motivate the development of new delivery strategies.

Materials and methods that provide spatial and temporal control over the localized release of therapeutic agents play significant roles in the development of localized therapies. Until now, immobilization materials for tunable DNA delivery are mainly cationic polymers for they can self-assemble with DNA to form particles or films that are capable of being endocytosed by cells [20]. Other inorganic compounds have not been extensively studied. In particular, LbL films of inorganic compound and DNA have not been reported in tunable gene delivery. A major obstacle for their practical application is the poor biocompatibilities or even biotoxicities under certain circumstance. Recently, polyoxometalates (POMs) have been explored as a kind of therapeutic agent for their promising antiviral, antitumor activities [21]. And the zirconium compounds, especially zirconium citrate, have been used to remove radioelements from the mammalian body due to their comparably better biocompatibilities [22–24]. Several zirconium complexes have been tested for activity against respiratory syncytial virus and cancer [25]. A new capillary coating of zirconium phosphate/lysozyme multilayer film has been fabricated for open-tubular electrochromatography enantioseparation [26]. We have constructed Zr^{4+}/DNA multilayer films through LbL assembly of Zr^{4+} and DNA. The film provides a favorable biocompatible microenvironment for immobilizing biomolecules and preserves the bioactivity of biomolecules [10]. It is demonstrated that chelator coordinates with inorganic ions and plays an important role in the regulation of various physiological processes [27]. In most pharmacological applications, i.e., chelation therapy, chelator is used to enhance the excretion of heavy metal ions or provide trace elements in nutrient media [28]. Based on these findings, we hypothesize that chelator may provide a specific stimulus for controllable disassembly of DNA-incorporated LbL films.

The objective of the present study was to assess the possibility of disassembling the Zr^{4+}/DNA multilayer films and releasing the incorporated DNA by chelation. We envisaged that the Zr^{4+}-involved chelation could be reflected in its lower binding affinity for DNA, which was consequently released from the film surface. It was supposed that multiple and time-scheduled in situ gene delivery could be successfully carried out after the Zr^{4+}/DNA multilayer films were encapsulated in polyelectrolyte multilayer films [6]. The result of this work would have a significant impact on the development of localized gene therapies and open an alternative route to numerous potential applications. More importantly, some of the chelators can be obtained easily from foods, which suggest that this method was a promising new tool in dietetic therapy.

2. Experimental section

2.1. Materials and methods

All solutions were made with deionized water, which was further purified with a Milli-Q system (Millipore). Deoxyribonucleic acid (DNA, fish sperm, sodium salt), human serum albumin (HSA) and 11-mercaptoundecanoic acid (MUA) were obtained from Sigma. The following materials were purchased from Beijing Chemical Regent Co.: zirconyl chloride octahydrate ($ZrOCl_2{\cdot}8H_2O$), sodium fluoride, sodium acetate, sodium citrate, citric acid, sodium tartrate, ethylene diamine tetra-acetic acid (EDTA, disodium salt) and sodium chloride. All of the chemicals were of analytical grade and used as received. Dulbecco's modified Eagle's medium (DMEM) was obtained from HyClone Corp. (USA). Trypsin was obtained from Amresco (USA). Fetal bovine serum (FBS) was obtained from Gibco (USA). GeneFinder™ was purchased from Bio-v Company (China). Lipotap reagent was obtained from Beyotime Company (Jiangsu, China). Plasmid DNA (pDNA), pEGFP-C1 (4.9 kb, Clontech, Mountain View, CA, USA) was kept in *Escherichia coli* DH5α. Midipreps DNA Purification System was obtained from Promega Corp., USA. HEK 293 cells (human embryonic kidney cell line) were obtained from Kunming Institute of Zoology, Chinese Academy of Sciences.

2.2. Zr^{4+}/DNA multilayer film assembly and controllable disassembly

Quartz slides, silicon wafers and surface plasmon resonance (SPR) gold thin films were used as template substrates to assemble the multilayer films. Quartz slides and silicon wafers were rinsed with Milli-Q water and ultrasonically cleaned with subsequently warm (30 °C) ethanol and dichloromethane. These two substrates were cut into 5×10 and 10×25 mm^2 respectively, and then they were treated with piranha solution (3:7 mixtures of 30% H_2O_2 and 98% H_2SO_4) for 30 min at 60–70 °C, washed several times with Milli-Q water, ultrasonically treated with a mixture of HCl (37%)/H_2O (1:6 v/v) for 30 min, thoroughly rinsed with large amounts of Milli-Q water again, and ultrasonically cleaned with methanol, a methanol/toluene (1:1 v/v) mixture and toluene for 5 min. After these steps these substrates were blown dry with a strong flow of nitrogen and immediately used to construct the multilayer films. To assemble the multilayer films, gold thin films were preassembled with a self-assembled monolayer (SAM) of MUA by immersing it in 1 mM MUA ethanolic solution overnight. The Zr^{4+}/DNA multilayer films were deposited by alternately immersing the thiol-modified gold thin films in Zr^{4+} and DNA aqueous solutions. The overall assembly and disassembly procedures on gold thin films were schematically shown in Fig. 1. The first step depicted MUA anchoring on gold thin film surface (1). Subsequent assembly of the multilayer film was as follows: Successively incubating the activated substrates in fresh prepared 0.1 mM Zr^{4+} solution (pH 3.0, containing 0.1 M NaCl) for 5 min (2) and 0.1 mg/mL DNA solution (pH 3.0, containing 0.1 M NaCl) for 5 min (3), with intermediate pure water rinsing. Each bilayer referred to one Zr^{4+} layer and one DNA layer. This process was repeated until the desired number of bilayers was achieved. By incorporating fish sperm DNA and plasmid DNA (pDNA) into the multilayer films, they were designed respectively as $(Zr^{4+}/DNA)_n$ films and $(Zr^{4+}/pDNA)_n$ films, where n was the bilayer number. Unless mentioned, these films built with DNA as the outermost layer. The chelation-based disassembly of the films was performed in chelator aqueous solution (4), and the process was monitored in situ by SPR. Films used in AFM and UV–vis characterization were dried under a stream of nitrogen, placed in a desiccator and stored dry until use.

2.3. Electrophoretic mobility shift assay (EMSA) and cell transfection assay

EMSA was used to characterize the integrity of the released pDNA during the tunable DNA release experiment. The $(Zr^{4+}/pDNA)_{11}$ film was disassembled by incubating in 5 mM sodium citrate solution for 1 h. The disassembly trigger solution was exchanged for four times with fresh trigger solution at the end of each time period (1 h). EMSA was performed by loading the above treated pDNA samples into 1.0 wt.% agarose gel and ran at 80 V for approximately 1 h. Afterwards, the gel was incubated in 1× GeneFinder solution for 4 h. Then the gel was photographed under UV light using a Vilber Lourmat Fluorescent Gel Imaging and Analysis System.

HEK 293 cells were cultured in DMEM, supplemented with 10% fetal bovine serum (FBS) at 37 °C in a humidified 5% CO_2 incubator. The cells were seeded to a 96-well plate and incubated overnight. The wells were 60–80% confluent on the day of transfection. After the $(Zr^{4+}/pDNA)_{11}$ film was disassembled by using 5 mM sodium citrate solution just as in the case of EMSA experiment, four parts of the released pDNA were applied directly in Lipotap mediated transfection experiment, which was performed according to the manufacturer's instructions (Beyotime Company, China). After transfection, the cells were allowed to grow for another 48 h in the incubator. At that time, culture wells were usually

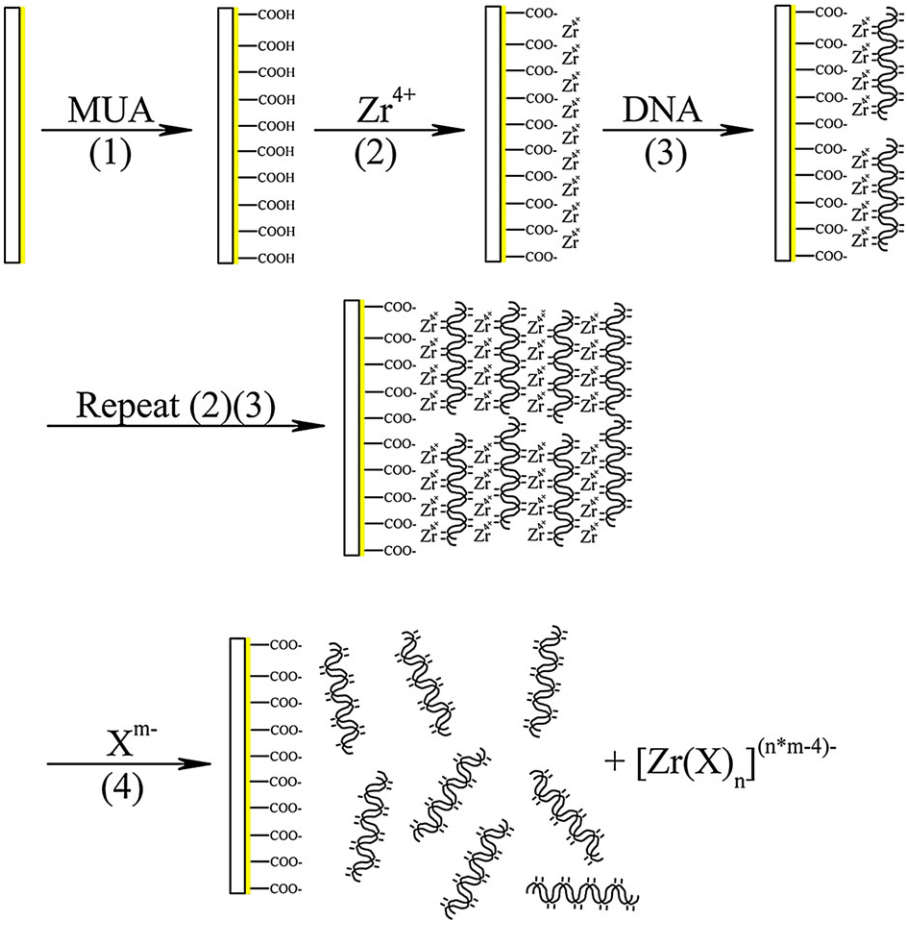

Fig. 1. Schematic of the layer-by-layer assembly and the disassembly of Zr^{4+}/DNA multilayer films. Here *X* and *m* represent respectively the chelator and its charge number, while *n* represents the number of chelator in the resultant coordination compound. The coordination compound is simplified as a mononuclear compound for clarity. The scheme does not indicate the real DNA structure and the topographic feature of the multilayer films.

100% confluent. The fluorescence images were taken using a confocal laser scanning fluorescence microscope (CLSM, Leica TCS SP2).

2.4. Apparatus and measurements

UV–vis absorption spectra were recorded using a Cary 500 UV–vis–NIR spectrometer (Varian). Real-time SPR measurements were conducted by using a home-built SPR system. Details of this setup had been described previously [10,29]. The exposed gold surface area was 0.8 cm^2. The volume of reaction cell was 0.5 mL for in situ SPR measurement and 0.05 mL for EMSA and cell transfection experiments. The film morphologies on silicon wafer were acquired in tapping mode atomic force microscopy (AFM) under ambient conditions (Nanoscope a; Digital Instruments, Inc.). Si_3N_4 cantilevers having integral tips (Spring contact, 20–100 N/m) were used. The images were obtained by oscillating the cantilever slightly below its resonance frequency (typically, 200–300 kHz) and raster scanning across the surface.

3. Results and discussion

3.1. Characterization of LbL film assembly

3.1.1. UV–vis spectrometry study of the LbL film assembly

The LbL assembly of Zr^{4+}/DNA multilayer films was monitored by UV–vis spectrometry. Fig. 2 shows the UV–vis absorption spectra of the assembled films with increasing number of bilayers on a quartz surface. Because Zr^{4+} has no apparent absorption in the wavelength range of 200–600 nm, the absorption maximum observed at 262 nm is the characteristic band of DNA absorption, which agrees well with previously reported absorption spectra [18]. Plot of the absorbance of DNA layer at 262 nm against the number of bilayers demonstrates a linear relationship up to 11 bilayers (Fig. 2, inset), indicating that the films are uniformly assembled by the LbL technique. This makes the precise controlling the amount of deposited gene materials possible

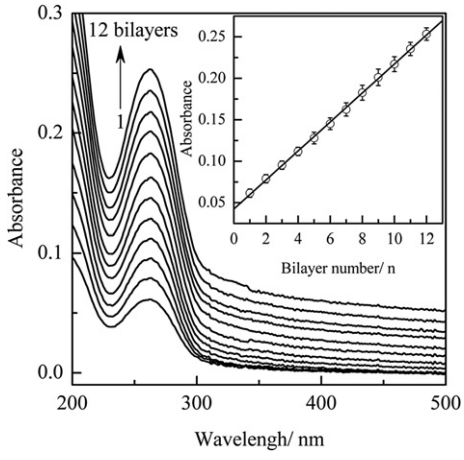

Fig. 2. UV–vis absorption spectra of $(Zr^{4+}/DNA)_n$ films with increasing number of bilayers on quartz slide. The inset is the plot of the absorbance of $(Zr^{4+}/DNA)_n$ films at 262 nm against the number of bilayers.

simply by controlling the number of bilayers. The driving force for the construction of $(Zr^{4+}/DNA)_n$ film is derived from the strong ionic coordinative interactions between Zr^{4+} and phosphate groups of DNA [30].

3.1.2. Surface plasmon resonance (SPR) study of the LbL film assembly

The SPR technique is extremely sensitive to the refractive index of layer presented in the interfacial region [31], and it is applied to investigate the construction of the LbL films recently [10]. Here, we use SPR spectroscopy to characterize the assembly of Zr^{4+}/DNA multilayer films. Two approaches were taken to monitor the construction of the films. First, the molecule/ion adsorption kinetics was followed by tracking the reflectance (R) at a fixed resonance angle near the θ_{SPR} with time ($R-t$ mode measurement), molecule/ion adsorption giving rise to positive shifts in R. Second, after each molecule/ion assembly and water rinsing step, angular reflectance curves were recorded and fitted to a multilayer Fresnel model to obtain the optical film thickness with increasing number of bilayers ($R-\theta$ mode measurement).

The in situ $R-t$ mode measurement was used for observing adsorption kinetics to establish the time for adsorption saturation. Fig. 3(a) shows in situ SPR kinetic curves of successive Zr^{4+}(Z1) and DNA (D1) adsorption for the first bilayer. A rapid increase in SPR reflectance, which reaches a constant value after 5 min, is observed upon injection of Zr^{4+} or DNA solution. Thus, a 5 min adsorption period provides saturation and is used in every cycle. Flushing the SPR cell with deionized water results in a small decrease in SPR reflectance. The reflectance change is attributed to the desorption of weakly adsorbed Zr^{4+} or DNA from the surface and the refractive index variation of the solution. The in situ $R-t$ mode measurement was also used to quantitatively monitor the alternate assembly of the Zr^{4+}/DNA multilayer films. Kinetic curves recorded for the films show a stepwise increase in SPR reflectance with each successive deposition of Zr^{4+} and DNA, demonstrating that a layer of Zr^{4+} and a layer of DNA are alternatively adsorbed to form the multilayer films. Plot of the SPR reflectance change against the bilayer number shows a linear relationship up to 11 bilayers (Fig. 3(b)), which is consistent with UV–vis spectrometry measurement. Thus, it is possible to monitor, in situ, the subsequent disassembly of the films quantitatively by $R-t$ mode measurement under various conditions.

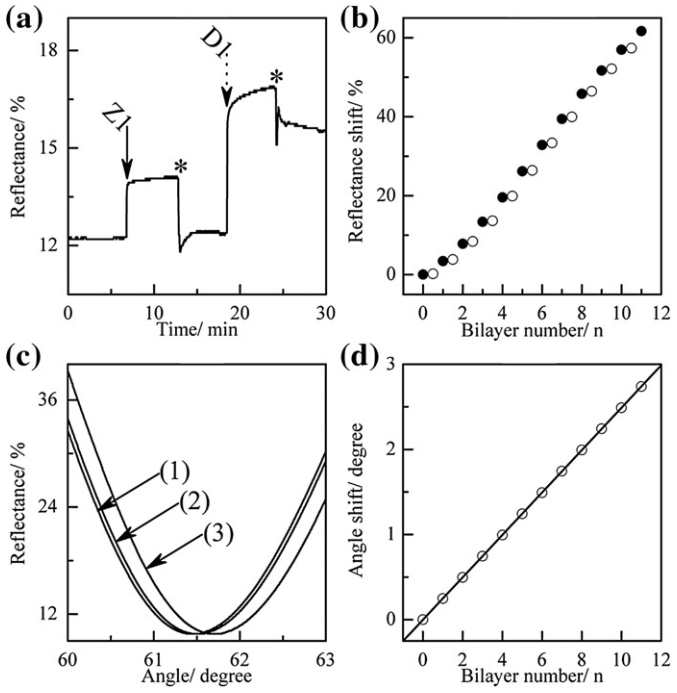

Fig. 3. (a) SPR $R-t$ mode monitoring of in situ kinetics of Zr^{4+} assembled onto MUA modified gold thin film and the subsequent adsorption of DNA on Zr^{4+} upon immersion of gold thin film into separate solutions. SPR angle is fixed at 61° and keeps unchanged during the construction of the Zr^{4+}/DNA multilayer films. Solid black arrows indicate the injection of Zr^{4+} solution. Dot black arrows indicate the injection of DNA. The black stars point to the injection of deionized water. (b) Shifts in the SPR reflectance as a function of the number of bilayers after the deposition of Zr^{4+} (open symbols) and DNA (filled symbols). The suffix n indicates the number of bilayers and half means the outermost layer is Zr^{4+}. (c) In situ scanning SPR curves of Zr^{4+} layer (2) and DNA layer (3) sequential adsorption onto a MUA (1) modified gold thin film. (d) Correlation of changes of SPR angle shift ($\Delta\theta$) with increasing number of bilayers.

The $R-\theta$ mode measurement was applied to quantify the deposited DNA of each bilayer and shown in Fig. 3(c). After formation of the first Zr^{4+} layer, SPR angle right shifts by ca. 0.03° in comparison to the basal surface. Upon saturation adsorption of the DNA layer to positively charged Zr^{4+} surface, another right-shift of SPR angle, $\Delta\theta$=0.22°, occurs. The DNA layer thickness d_{DNA}=1.8±0.1 nm is obtained from a numerical calculation based on Fresnel optics model involving four phase: a ZK_7 lens (n=1.61), a gold film (n=0.47+4.07i and thickness d=44 nm), DNA layer (n=1.5), and a buffer (n=1.3301). The effective thickness value of DNA monolayer is somewhat larger than that of our earlier report [10], but is reasonable because of the different assembly conditions. Taking into account the double-stranded DNA diameter of 1.9 nm, we conclude that the surface coverage of each DNA layers is 95% of its full packed monolayer. SPR angle shift of Zr^{4+} and DNA follows the same general trend for each bilayer. The $R-\theta$ mode measurement was further used to investigate the assembly of the Zr^{4+}/DNA multilayer films. SPR angle shift is observed to increase linearly with the bilayer number as shown in Fig. 3(d). So a regular and uniform film is constructed, according well with the above results obtained from UV–vis absorption spectroscopy and in situ $R-t$ mode measurement. Moreover, the film density (the ratio of DNA amount to film thickness calculated from data in Figs. 2 and 3) nearly unchanges with increasing number of bilayers, implying a strong ionic coordinative interaction between Zr^{4+} and phosphate groups of DNA inside the films. It also demonstrates the favorable stability of the multilayer films.

3.1.3. AFM study of the LbL film assembly

AFM was used to characterize the surface topographic features of the LbL films. The AFM micrographs of $(Zr^{4+}/DNA)_n$ films with 2, 4, 6, 8 and 10 bilayers are shown in Fig. 4. The surface of silicon wafer is decorated with many island-like objects, which is considered to be the assembled Zr^{4+}/DNA complex. The shape of DNA molecules assembled on silicon wafers is circular (with the diameter of 30–50 nm), suggesting that the DNA strands have folded into coiled conformations. On the other hand, it might confirm the effect of pH [32] or/and ionic strength [33] on the conformation of DNA molecules though the effect of Zr^{4+} cannot be neglected. At the early stages of the film assembly, small islands are seen with a characteristic height of 2–3 nm, which is consistent with the width of a double-stranded DNA molecule. For the case of the $(Zr^{4+}/DNA)_2$ films, our results are quite similar to those obtained by Zhou et al. [34]. During the initial stage of the multilayer film construction, i.e. bilayer number 2–6, the density of the island-like domains increases without changing their size. However, this situation changes as the build up continuing, i.e., bilayers 8–10, larger island-like domains prevail and small holes disappear. The larger island-like domains (with the diameter of 80–100 nm) might be derived from the collapse of the small island-like domains. The root mean square (RMS) roughness increases from 2.1 to 13.4 nm during the whole process.

3.2. Characterization of LbL film disassembly

3.2.1. SPR study of the chelation-based film disassembly

Precise control over the gene delivery is highly desirable for optimizing gene therapy and the gene release profile is expected to be different depending on its application. For example, the disease of

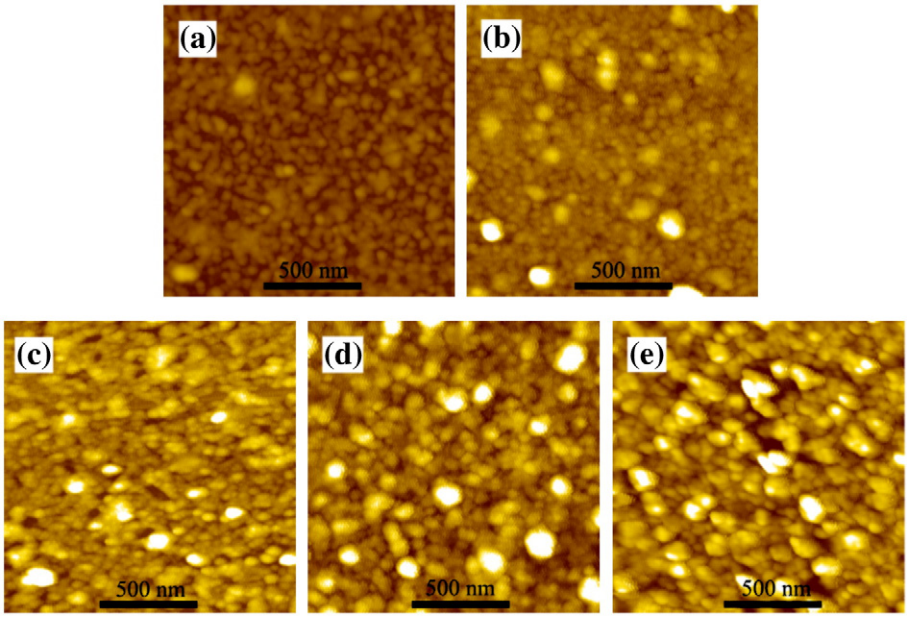

Fig. 4. AFM topography images (1500 nm × 1500 nm) of the $(Zr^{4+}/DNA)_n$ films with 2, 4, 6, 8, and 10 (a–e, respectively) bilayers. The outermost layer is DNA and the maximum height or *z*-range is 35 nm.

gene dysfunction like hypercholesterolemia needs a prolonged and sustained gene expression, while in the case of most cancer gene therapy strategies, a short period of gene expression is sufficient [35]. So a gene delivery system with tunable DNA release kinetics is important for its clinical application. The disassembly of $(Zr^{4+}/DNA)_n$ films was carried out in various chelator solutions and monitored in situ by SPR. Unless mentioned, SPR response caused by the refractive index variation of solution has been subtracted in the $R-t$ mode measurement. A relative reflectivity of 100% represents the existence of original $(Zr^{4+}/DNA)_{11}$ films, while 0% designates the MUA modified SPR gold thin films. We assumed that the coordinative/electrostatic interactions between Zr^{4+} and phosphate groups in the backbone of the DNA chain would be cleaved by chelation. With higher affinity, the chelator can substitute the phosphate groups of DNA by reacting with Zr^{4+}. The resultant coordination compounds would then release from the multilayer films, leading to the subsequent disassembly of DNA-incorporated LbL films. This substituent reaction has been confirmed theoretically and experimentally by studying the affinity of chelating group to Zr^{4+} and the coordinating tendency varies as $RO^- > RCOO^- > ROR > R_3N > (RO)_3P \gg RS^-$ [27]. Then carboxylic acid group is chosen as the disassembly trigger because it has a large variety of derivatives with good biocompatibility and extensive applications in daily life. Moreover, the dissociated carboxylic group might react with Zr^{4+} to form an anionic coordination compound under a certain condition, which conduces to the disassembly of Zr^{4+}/DNA multilayer films via electrostatic repulsion.

The disassembly of the $(Zr^{4+}/DNA)_{11}$ films was first investigated in various chelator solutions at a fixed concentration (5 mM) by $R-t$ mode measurement. The declined SPR reflectance reflects the relative disassembly capabilities of chelators for the films. With this approach, we examined a set of chelators that is probably allowed for tunable DNA release. An appropriate chelator was first screened out from three commonly used sourness/food additive: sodium acetate, sodium citrate and sodium tartrate, and two well-known chelators: EDTA and sodium fluoride. As shown in Fig. 5(a), no significant disassembly of the films is observed in 0.15 M NaCl solution alone, which indicates that the Zr^{4+}/DNA multilayer films are rather stable. The stability of the multilayer film in HSA solution (0.1 mg/ml) is different from that in NaCl solution (0.15 M). The unusual features for zirconium (IV) binding to human serum protein make it possible that HSA adsorbs on the film and then slightly disassembles the film [36]. As predicted, the $(Zr^{4+}/DNA)_{11}$ films disassemble easily and release continuously the incorporated DNA in the presence of some chelators. The disassembly profile shows an exponential decrease and is quite different in various chelators. For example, about 97% of the film is released in 6 h in the presence of sodium citrate, compared with 86% of the films in 6 h in sodium tartrate, 70% of the films in 6 h in sodium fluoride, and 17% of the films in 15 h in sodium acetate. The results imply that the disassembly capabilities of chelators vary as sodium citrate > sodium tartrate > sodium fluoride > sodium acetate although other factors should also be considered, such as pH, hydrophobic interactions, and solubility of the resultant coordination compounds. Considering their disassembly capabilities and biocompatibility, sodium citrate is chosen as the disassembly trigger in the following experiments. It is very interesting to find that EDTA, the most effective and commonly used sequestering chelator for heavy metal ions, cannot disassemble the films even in high concentration (~250 mM). It might be attributed to the neutral or even positive charges of the resultant EDTA–Zr^{4+} coordination compounds because the ratio of EDTA to Zr^{4+} is usually 1:1 in coordination reaction [37]. The coordination compounds composed of other chelators and Zr^{4+} might be negatively charged, and their coulomb repulsion with negatively charged DNA considerably contributes to the controlled release of DNA from the LbL films.

The influence of chelator concentration and ionic strength on the disassembly of the $(Zr^{4+}/DNA)_{11}$ films was also studied. Taking sodium citrate as an example, the disassembly profile of the film in different concentrations of sodium citrate solution is plotted in Fig. 5(b). The half release time $t_{1/2}$, at which half of the film has been released, is 1, 3, 6, 11 and more than 15 h for sodium citrate with the concentrations of 10, 3, 2, 1 and 0.5 mM, respectively. The results indicate that $t_{1/2}$ can be prolonged to more than 15 times so long as the concentration of sodium citrate is simply decreased from 10 to 0.5 mM. Thus, the release of DNA could be easily accelerated though increasing the concentrations of sodium citrate. This concentration dependent disassembly profile is attributed to the fact that higher concentration of chelator induces higher coordination reaction rate and the consequential disassembly rate. The ionic strength is the same as

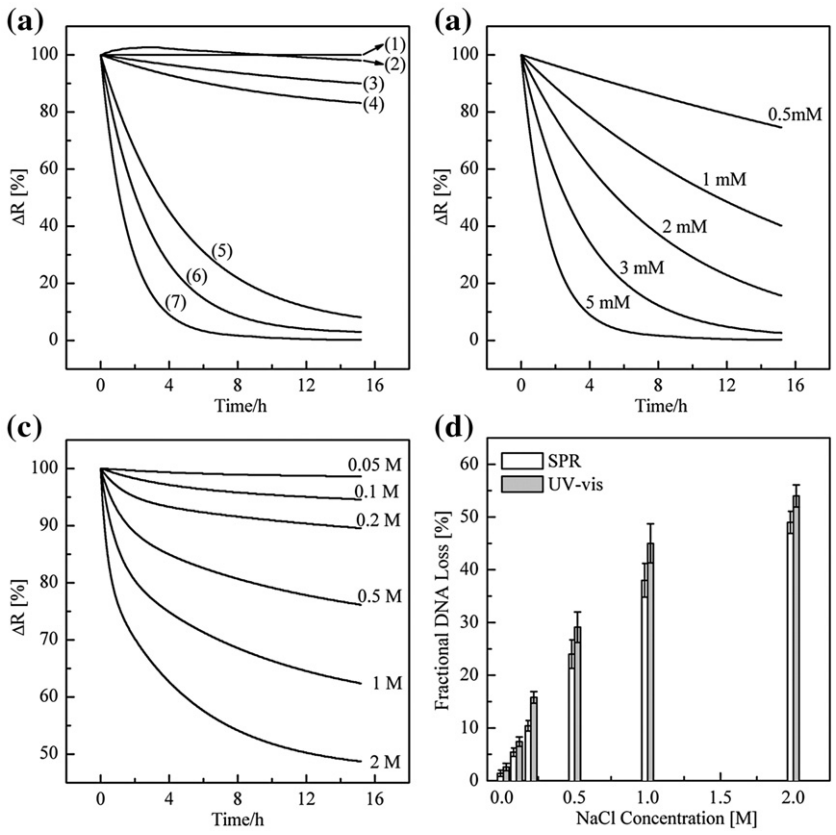

Fig. 5. (a) SPR $R-t$ monitoring of DNA release kinetics from the $(Zr^{4+}/DNA)_{11}$ films by incubating in various chelators: (1) 250 mM EDTA; (2) 0.1 mg/ml HSA; (3) 150 mM NaCl; (4) 5 mM sodium acetate; (5) 5 mM sodium fluoride; (6) 5 mM sodium tartrate; and (7) 5 mM sodium citrate. SPR $R-t$ monitoring of DNA release from the $(Zr^{4+}/DNA)_{11}$ films by incubating in different concentration of sodium citrate (b) and NaCl (c). The fixed angle is 61° and the angle position holds unchanged. A relative reflectivity of 100% represents the existence of original $(Zr^{4+}/DNA)_{11}$ film, while 0% designates the MUA modified gold thin films. (d) The fractional DNA loss as a function of the NaCl concentration of the incubation solution. SPR and UV–vis spectroscopy were used to investigate the salt induced deconstruction of the films in 15 h.

the formal concentration for a 1:1 electrolyte such as NaCl, which is then used interchangeably to describe the effect of ionic strength on the disassembly of the $(Zr^{4+}/DNA)_{11}$ films. In fact, this disassembly mechanism is also (at least partly) derived from the coordination interactions. We emphasize it in this section because some special organs or tissues (such as kidney) have the higher ionic strength than normal physiological ionic strength. It is necessary to investigate the stability or disassembly of the Zr^{4+}/DNA multilayer films in solution with different ionic strength. As shown in Fig. 5(c), the films are disassembled upon incubated in higher concentration of NaCl solution and the extent of disassembly varies with the ionic strength. For instance, 10% and 51% of the film has been released after an incubation of 15 h in 0.1 and 2 M NaCl solution, respectively. It is consistent with UV–vis result (Fig. 5(d)). Two reasons might be responsible for this phenomenon. One is the shielding action of salt ions on phosphate groups of DNA [33], resulting to the depletion of electrostatic attraction. Another is the coordination action of chloride ions, which would coordinate with Zr^{4+} in the multilayer films and weaken or break the interaction between Zr^{4+} and DNA molecules. Then the films disassemble and release the incorporated DNA. The disassembly of the films is somewhat different as compared to that of polymer/DNA multilayer films in mechanism and could be served as an alternative localized gene delivery system.

3.2.2. AFM study of the chelation-based film disassembly

AFM was used to periodically gain information about the topographical changes of the multilayer films during the disassembly process. The $(Zr^{4+}/DNA)_{11}$ films in 5 mM sodium citrate solution were followed over a period of 4 h by AFM (Fig. 6). As mentioned above, the original $(Zr^{4+}/DNA)_{11}$ film surface before injection of the disassembly trigger (sodium citrate) solution contains island-like aggregates with diameter in 30–100 nm. The morphology of the multilayer film surface changes obviously after a 10 min immersion in sodium citrate solution. As shown in Fig. 6(b), many "gaps" are present while larger particulate aggregates disappear or blur in edge. The larger islands continue to decrease in density and break apart by the inserted "gaps" after 20 min (Fig. 6(c)). Most of the larger particles have been removed from the surface after 30 min of incubation in sodium citrate solution. (Fig. 6(d) and (e)). Then smaller particles start to erode and disappear after 4 h (Fig. 6(f)). The removal of larger particles at the first stage of the disassembly accords very well with the initial exponential disassembly of the films as larger particles contribute to large decrease in thickness. The roughness of the $(Zr^{4+}/DNA)_{11}$ films shows a smaller change after the first 30 min, implying at least partially a subsequent disassembly profile of LbL removal.

3.2.3. Electrophoretic mobility shift assay (EMSA) and cell transfection assay of the released DNA

As an important prerequisite for gene delivery, the released DNA should preserve its integrity and bioactivity. It is necessary to evaluate the released DNA by performing EMSA and transfection experiment. As is well known to all, fish sperm DNA typically has fairly low molecular weight and broad molecular weight distribution, and it is not transcriptionally active when administered to mammalian cells. Then we selected a commercially available, supercoiled pDNA construct encoding for enhanced green fluorescent protein (pEGFP-C1, 4.9 kb) in the subsequent experiments. This pDNA is well defined and monodisperse and can serve as a reporter gene in cell transfection

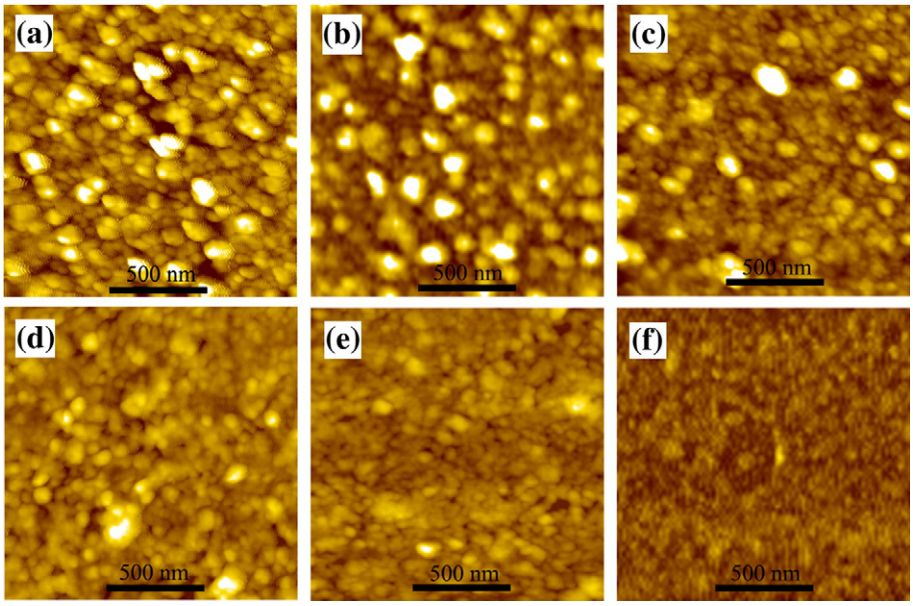

Fig. 6. AFM topography images (1500 nm× 1500 nm) of the $(Zr^{4+}/DNA)_{11}$ films after 0, 10, 20, 30, 90 and 240 min (a–f, respectively) of disassembly in 5 mM sodium citrate aqueous solution. The maximum height or *z*-range is 35 nm.

experiment. To show the difference between fish sperm DNA and plasmid DNA, SPR, UV–vis spectroscopy and AFM were applied to monitor the assembly and disassembly of the $(Zr^{4+}/pDNA)_{11}$ films (Fig. 7). The $(Zr^{4+}/pDNA)_{11}$ films are rather uniform as demonstrated by SPR. They have higher surface coverage of DNA at a given bilayer number than the $(Zr^{4+}/DNA)_{11}$ films (Fig. 7(A)). It is attributed to the molecular weight and molecular weight distribution difference between fish sperm DNA and plasmid DNA. SPR was further applied to study the disassembly of $(Zr^{4+}/pDNA)_{11}$ films in 5 mM sodium citrate solution. To acquire more detailed information on tunable DNA

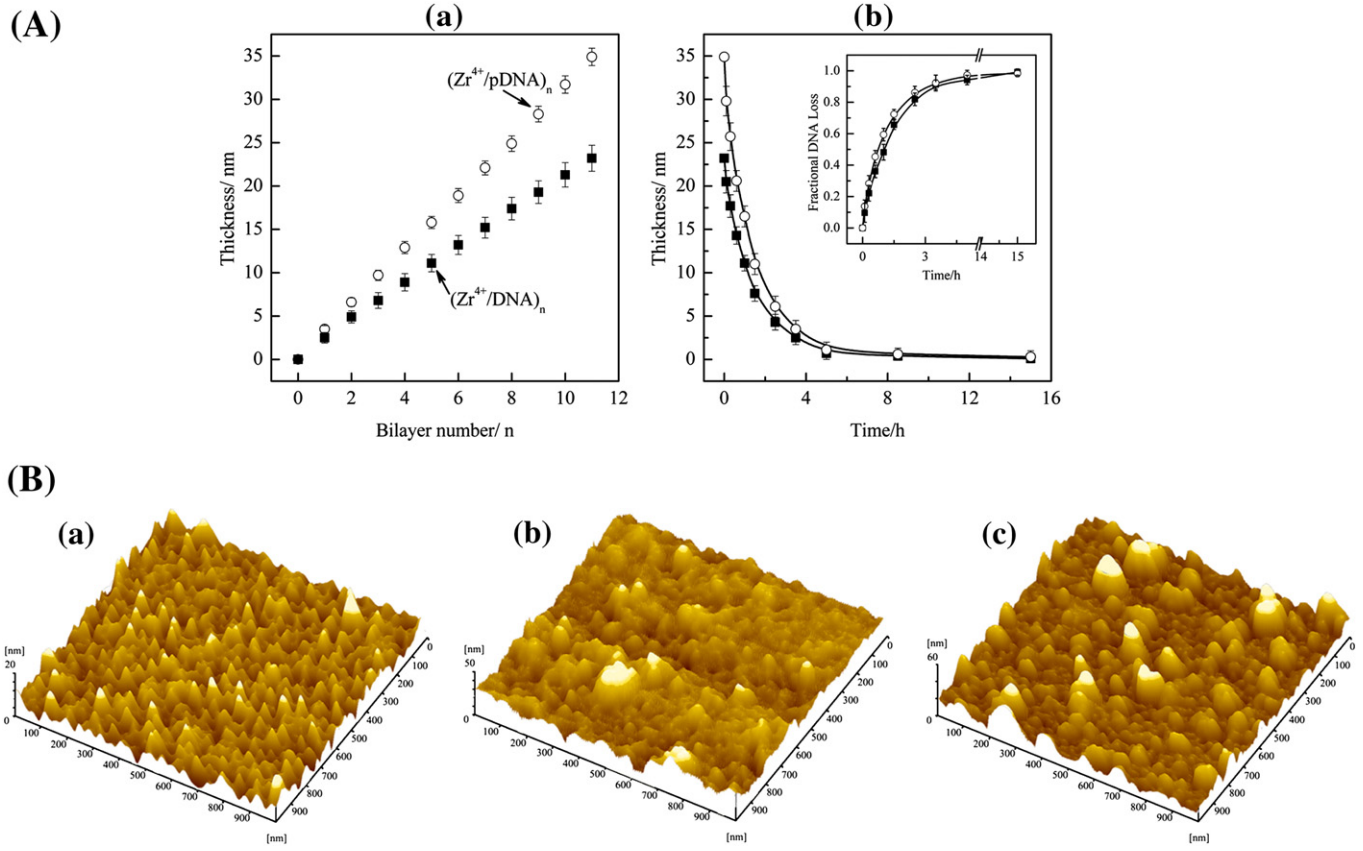

Fig. 7. (A) Thickness of the Zr^{4+}/DNA (■) and Zr^{4+}/pDNA (○) multilayer films as a function of the bilayer number (a) and the thickness of multilayered films decreased as a function of disassembly time (b) as determined by SPR. Inset of (b) shows the UV–vis spectroscopy monitoring the released DNA in 5 mM sodium citrate solution. (B) AFM topography images of the surfaces of $(Zr^{4+}/pDNA)_n$ films with 4, 8, and 11 (a–c, respectively) bilayers.

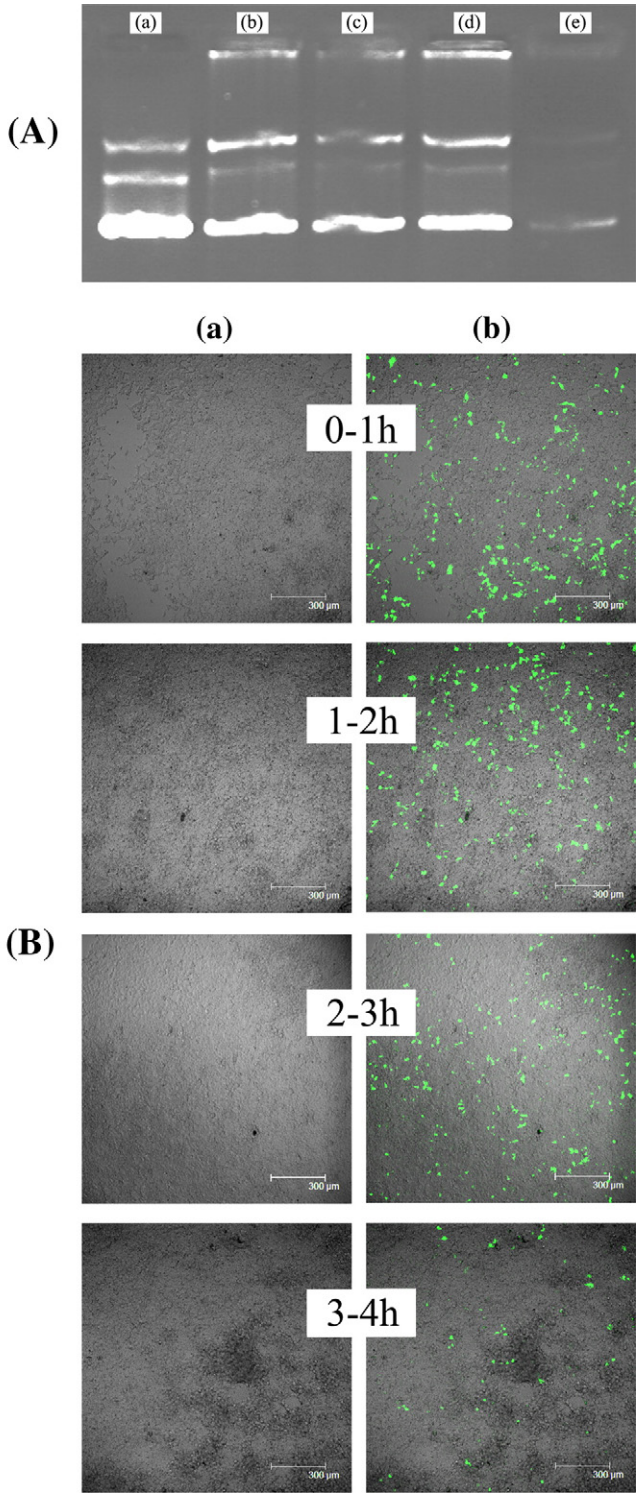

Fig. 8. (A) The agarose gel electrophoresis of the released plasmid DNA in 5 mM sodium citrate solution. As described in the text, plasmid DNA is collected in four discrete batches with the same duration of 1 h. The intensity of the white GeneFinder stained bands correspond to amounts of plasmid DNA released and collected over each of the following time periods: (b) 0–1 h, (c) 1–2 h, (d) 2–3 h, (e) 3–4 h. Lane (a) corresponds to pure plasmid DNA as a reference. (B) The CLSM images of HEK293T cells: Phase-contrast image (a) and fluorescence image (b) of the transfected cells (adding DNA sample). The selected overlay CLSM images of EGFP fluorescence and bright field of HEK 293 cells are shown with 300 mm scale bars. The samples are transfected with plasmid DNA released from $(Zr^{4+}/pDNA)_{11}$ film by incubating 5 mM sodium citrate over the indicated time periods. Lipotap are mixed firstly before DNA is added, then the mixture is used for transfection.

release, UV–vis spectroscopy was used as a complementary technique to determine the released pDNA in 5 mM sodium citrate solution. They show the same disassembly trend as illustrated before, demonstrating that most of the films have been disassembled in 4 h, which is analogous with that of the $(Zr^{4+}/DNA)_{11}$ films. In addition, AFM characterization of the $(Zr^{4+}/pDNA)_n$ films shows that the films are rather uniform at the beginning and then prevailed by larger island-like domains during the assembly process (Fig. 7(B)). The films have the same trend of topographical changes as the $(Zr^{4+}/DNA)_n$ films. It is supposed that Zr^{4+} can be used as a condensing agent for DNA condensation, which normally requires cations of charge +3 or greater in aqueous solution [38]. As an inorganic quadrivalent cation, Zr^{4+} might be also used as a condensing agent for gene delivery and condenses DNA on the surface, resulting in the topographical changes of the films. Actually, metal ions induced DNA condensation has been applied to prepare metal–DNA nanohybrid structures recently [39].

EMSA was carried out to characterize the released DNA in sodium citrate solution. Fig. 8(A) shows EMSA of pDNA that was taken from the disassembly of $(Zr^{4+}/pDNA)_{11}$ film periodically in 5 mM sodium citrate solution. It demonstrates that pDNA is released without any damage by disassembly trigger (sodium citrate solution), because the released pDNA migrates to the same position of the original pDNA. Thus, this chelation-based localized gene delivery has realized the consecutive pDNA release without appreciable structural changes. The retained pDNA in electrophoresis well is might attributed to the presence of Tris–borate–EDTA buffer (electrophoresis buffer) in EMSA experiment. To testify whether the released pDNA retained its transcriptional activity or not, we performed gene expression assay on HEK 293 cells with the assistance of Lipotap, a commercially available lipid-based transfection reagent. The disassembly experiment was the same as that in EMSA. The efficient transfection generally requires an auxiliary gene transfer agent, such as Lipotap or a cationic polymer-based delivery system, which self-assembles plasmid DNA into condensed nanostructures to enhance cellular uptake [20]. However, the use of noncomplexed plasmid DNA to transfect cells and tissue in vivo is well precedented [40]. The immobilization of DNA or DNA/vector complexes on surfaces has been used to increase the internalization of DNA by cells and promote surface-mediated transfection in vitro [41]. Fig. 8(B) shows fluorescence microscopy images of HEK 293 cells transfected with plasmid DNA collected over several different 1 h time periods during the incubation of $(Zr^{4+}/pDNA)_{11}$ film in 5 mM sodium citrate solution. The large number of cells expressing EGFP in these images demonstrates that pDNA is released from the $(Zr^{4+}/pDNA)_{11}$ film and retains a high transcriptional activity. The result is consistent with that of EMSA experiment.

The concentration of pDNA in the disassembly trigger solution depicted in Fig. 8 does not reflect cumulative concentration of the released pDNA, but the relative amounts of pDNA released from the film over four sequential, discrete time periods. The disassembly trigger (sodium citrate solution) was exchanged with the same volume fresh trigger at the end of each time period. Both of the EMSA and cell transfection assay demonstrate that the release of pDNA is sustained over a period of 4 h, which is consistent with SPR and UV–vis experiments. It is hoped that this approach would play a significant role in the development of new gene-based therapies.

4. Conclusions

In this paper, we present an initial study of tunable DNA release from Zr^{4+}/DNA multilayer films fabricated by LbL assembly. Chelator was used as an effective disassembly trigger by chelating Zr^{4+} into coordination compounds and cleaving the coordinative/electrostatic interactions between Zr^{4+} and phosphate groups of DNA. EDTA, a power chelator for Zr^{4+}, could not disassemble the films, indicating that the charge of the resultant coordination compounds was also an

indispensable factor. The assembly and disassembly of the multilayer films were monitored by SPR, UV–vis spectrometry and AFM. In addition to the advantages of the flexibility and versatility of the LbL films in implants and tissue engineering, the Zr^{4+}/DNA films offered additional benefits in tunable gene delivery as the film disassembly could be tuned locally by changing the chelator and ionic strength. EMSA and cell transfection assay were used to characterize the bioactivity of the released pDNA when incorporating pDNA into this controllable disassembly system. It was demonstrated that the released pDNA retained its integrity and high transcriptional activity, and also expressed the reporter protein after being transfected into HEK 293 cells. The most important advantage of this strategy was that the Zr^{4+} could be chelated by a large variety of chelators and the resulting coordination compounds were considered to be biologically inert. Some of the chelators were easily obtained from foods (e.g., tartaric acid of grape and citric acid of lemon), this method, in combination with electrochemistry, was a promising new tool in gene therapy and dietetic therapy. Although the potential biotoxicities of zirconium and its coordination compounds were still unknown [42], the present work could be used as a supplement technique to the controlled administration of therapeutic DNA, protein and drugs.

Acknowledgment

This work was supported by the special funds for major state basic research of China (No.2002CB713803) and the National Nature Science Foundation of China (No.20675076).

References

[1] A. Meager, Gene Therapy Technologies, Applications and Regulations, John Wiley & Sons, Ltd, 1999.
[2] G. Decher, Fuzzy nanoassemblies: toward layered polymeric multicomposites, Science 277 (5330) (1997) 1232–1237.
[3] N. Jessel, F. Atalar, P. Lavalle, J. Mutterer, G. Decher, P. Schaaf, J.C. Voegel, J. Ogier, Bioactive coatings based on a polyelectrolyte multilayer architecture functionalized by embedded proteins, Adv. Mater. 15 (9) (2003) 692–695.
[4] N. Benkirane-Jessel, P. Lavalle, F. Meyer, F. Audouin, B. Frisch, P. Schaaf, J. Ogier, G. Decher, J.C. Voegel, Control of monocyte morphology on and response to model surfaces for implants equipped with anti-inflammatory agents, Adv. Mater. 16 (17) (2004) 1507–1511.
[5] A. Dierich, E. Le Guen, N. Messaddeq, J.F. Stoltz, P. Netter, P. Schaaf, J.C. Voegel, N. Benkirane-Jessel, Bone formation mediated by synergy-acting growth factors embedded in a polyelectrolyte multilayer film, Adv. Mater. 19 (5) (2007) 693–697.
[6] N. Jessel, M. Oulad-Abdeighani, F. Meyer, P. Lavalle, Y. Haikel, P. Schaaf, J.C. Voegel, Multiple and time-scheduled in situ DNA delivery mediated by beta-cyclodextrin embedded in a polyelectrolyte multilayer, Proc. Natl. Acad. Sci. U. S. A. 103 (23) (2006) 8618–8621.
[7] N. Benkirane-Jessel, P. Schwinte, P. Falvey, R. Darcy, Y. Haikel, P. Schaaf, J.C. Voegel, J. Ogier, Build-up of polypeptide multilayer coatings with anti-inflammatory properties based on the embedding of piroxicam–cyclodextrin complexes, Adv. Funct. Mater. 14 (2) (2004) 174–182.
[8] N. Benkirane-Jessel, P. Lavalle, E. Hubsch, V. Holl, B. Senger, Y. Haikel, J.C. Voegel, J. Ogier, P. Schaaf, Short-time timing of the biological activity of functionalized polyelectrolyte multilayers, Adv. Funct. Mater. 15 (4) (2005) 648–654.
[9] Y. Wang, A.S. Angelatos, F. Caruso, Template synthesis of nanostructured materials via layer-by-layer assembly, Chem. Mater. 20 (3) (2008) 848–858.
[10] J. Wang, F. Wang, Z. Xu, Y. Wang, S. Dong, Surface plasmon resonance and electrochemistry characterization of layer-by-layer self-assembled DNA and Zr^{4+} thin films, and their interaction with cytochrome c, Talanta 74 (1) (2007) 104–109.
[11] S.A. Sukhishvili, S. Granick, Layered, erasable, ultrathin polymer films, J. Am. Chem. Soc. 122 (39) (2000) 9550–9551.
[12] S.T. Dubas, J.B. Schlenoff, Polyelectrolyte multilayers containing a weak polyacid: construction and deconstruction, Macromolecules 34 (11) (2001) 3736–3740.
[13] F. Boulmedais, C.S. Tang, B. Keller, J. Voros, Controlled electrodissolution of polyelectrolyte multilayers: a platform technology towards the surface-initiated delivery of drugs, Adv. Funct. Mater. 16 (1) (2006) 63–70.
[14] C.L. Recksiedler, B.A. Deore, M.S. Freund, A novel layer-by-layer approach for the fabrication of conducting polymer/RNA multilayer films for controlled release, Langmuir 22 (6) (2006) 2811–2815.
[15] J. Wang, G. Rivas, M.A. Jiang, X.J. Zhang, Electrochemically induced release of DNA from gold ultramicroelectrodes, Langmuir 15 (19) (1999) 6541–6545.
[16] M. Jiang, W.W. Ray, B. Mukherjee, J. Wang, Electrochemically controlled release of lipid/DNA complexes: a new tool for synthetic gene delivery system, Electrochem. Commun. 6 (6) (2004) 576–582.
[17] C.M. Jewell, J. Zhang, N.J. Fredin, D.M. Lynn, Multilayered polyelectrolyte films promote the direct and localized delivery of DNA to cells, J. Control. Release 106 (1–2) (2005) 214–223.
[18] K.F. Ren, J. Ji, J.C. Shen, Construction and enzymatic degradation of multilayered poly-L-lysine/DNA films, Biomaterials 27 (7) (2006) 1152–1159.
[19] J. Blacklock, H. Handa, D.S. Manickam, G.Z. Mao, A. Mukhopadhyay, D. Oupicky, Disassembly of layer-by-layer films of plasmid DNA and reducible TAT polypeptide, Biomaterials 28 (1) (2007) 117–124.
[20] A.V. Kabanov, V.A. Kabanov, DNA complexes with polycations for the delivery of genetic material into cells, Bioconjug. Chem. 6 (1) (1995) 7–20.
[21] J.T. Rhule, C.L. Hill, D.A. Judd, Polyoxometalates in medicine, Chem. Rev. 98 (1) (1998) 327–357.
[22] V.H. Smith, Removal of internally deposited plutonium, Nature 181 (4626) (1958) 1792–1793.
[23] J. Schubert, Treatment of plutonium poisoning by metal displacement, Science 11 (105) (1947) 389–390.
[24] S.S. Ghosh A., TalukderG. , Zirconium: an abnormal trace element in biology, Biol. Trace Elem. Res. 35 (1992) 247–271.
[25] D.L. Barnard, C.L. Hill, T. Gage, J.E. Matheson, J.H. Huffman, R.W. Sidwell, M.I. Otto, R.F. Schinazi, Potent inhibition of respiratory syncytial virus by polyoxometalates of several structural classes, Antivir. Res. 34 (1) (1997) 27–37.
[26] L. Geng, T. Bo, H.W. Liu, N. Li, F. Liu, K. Li, J.L. Gu, R.N. Fu, Capillary coated with layer-by-layer assembly of gamma-zirconium phosphate/lysozyme nanocomposite film for open tubular capillary electrochromatography chiral separation, Chromatographia 59 (1–2) (2004) 65–70.
[27] M.M. Jones, Elementary Coordination Chemistry, Prentice-Hall, Inc., Englewood Cliffs, NJ, 1965.
[28] J.L. Stumpf, Deferasirox, Am. J. Health-Syst. Pharm. 64 (6) (2007) 606–616.
[29] X.F. Kang, Y.D. Jin, G.J. Cheng, S.J. Dong, In situ analysis of electropolymerization of aniline by combined electrochemistry and surface plasmon resonance, Langmuir 18 (5) (2002) 1713–1718.
[30] M.M. Fang, D.M. Kaschak, A.C. Sutorik, T.E. Mallouk, A "mix and match" ionic-covalent strategy for self-assembly of inorganic multilayer films, J. Am. Chem. Soc. 119 (50) (1997) 12184–12191.
[31] O.A. Raitman, E. Katz, I. Willner, V.I. Chegel, G.V. Popova, Photonic transduction of a three-state electronic memory and of electrochemical sensing of NADH by using surface plasmon resonance spectroscopy, Angew. Chem., Int. Ed. 40 (19) (2001) 3649–3652.
[32] E.R. Garrett, P.J. Mehta, Solvolysis of adenine nucleosides. I. Effects of sugars and adenine substituents on acid solvolyses, J. Am. Chem. Soc. 94 (24) (1972) 8532–8541.
[33] J. Li, C. Bai, C. Wang, C. Zhu, Z. Lin, Q. Li, E. Cao, A convenient method of aligning large DNA molecules on bare mica surfaces for atomic force microscopy, Nucleic Acids Res. 26 (20) (1998) 4785–4786.
[34] Y.L. Zhou, Y.Z. Li, Layer-by-layer self-assembly of multilayer films containing DNA and Eu^{3+}: their characteristics and interactions with small molecules, Langmuir 20 (17) (2004) 7208–7214.
[35] A. El-Aneed, An overview of current delivery systems in cancer gene therapy, J. Control. Release 94 (1) (2004) 1–14.
[36] W.Q. Zhong, J.A. Parkinson, M.L. Guo, P.J. Sadler, Unusual features for zirconium(IV) binding to human serum transferrin, J. Biol. Inorg. Chem. 7 (6) (2002) 589–599.
[37] H. Matsunaga, C. Kanno, H. Yamada, Y. Takahashi, T.M. Suzuki, Fluorometric determination of fluoride ion by reagent tablets containing 3-hydroxy-2'-sulfoflavone and zirconium(IV) ethylenediamine tetraacetate, Talanta 68 (3) (2006) 1000–1004.
[38] V.A. Bloomfield, Condensation of DNA by multivalent cations: considerations on mechanism, Biopolymers 31 (1991) 1471–1481.
[39] Y. Hatakeyama, M. Umetsu, S. Ohara, F. Kawadai, S. Takami, T. Naka, T. Adschiri, Homogenous spherical mosslike assembly of Pd nanoparticles by using DNA compaction: application of Pd-DNA hybrid materials to volume-expansion hydrogen switches, Adv. Mater. 20 (2008) 1122–1128.
[40] L.D. Shea, E. Smiley, J. Bonadio, D.J. Mooney, DNA delivery from polymer matrices for tissue engineering, Nat. Biotechnol. 17 (6) (1999) 551–554.
[41] I. Fishbein, S.J. Stachelek, J.M. Connolly, R.L. Wilensky, I. Alferiev, R.J. Levy, Site specific gene delivery in the cardiovascular system, J. Control. Release 109 (2005) 37–48.
[42] http://www.intox.org/databank/documents/chemical/zirc/ukpid90.htm and reference therein.